Available online at www.sciencedirect.com
SCIENCE DIRECT®
ELSEVIER
International Journal of Solids and Structures 42 (2005) 5555–5567
INTERNATIONAL JOURNAL OF SOLIDS and STRUCTURES
www.elsevier.com/locate/ijsolstr

Dynamic buckling of thin-walled composite plates with varying widthwise material properties

Tomasz Kubiak *

Technical University of Lodz, Department of Strength of Materials and Structures (K12), PL 90-924 Lodz, ul. Stefanowskiego 1/15, Poland

Received 19 February 2005
Available online 12 April 2005

Abstract

The paper deals with dynamic response of a thin-walled rectangular plate subjected to in-plane pulse loading. The plate is made of orthotropic (fibre composite) material in which the principal directions of orthotropy are parallel to the plate edges. The plate is characterised by a widthwise varying fibre volume fraction. The structures are assumed to be simply supported at the loaded ends and at non-loaded ends with five different boundary conditions (both simply supported, both fixed, simply supported fixed, simply supported free edge, fixed free edge). In order to obtain the equations of motion the non-linear theory of orthotropic thin-walled plates has been modified in such a way that it additionally accounts for all components of inertial forces. The differential equations of motion have been obtained from Hamilton's Principle. The problem of nonlinear static stability was solved with the second order of the Koiter's asymptotic stability theory of conservative systems. The results obtained from analytical–numerical method were compared with the results from finite element method (FEM).

Keywords: Dynamic buckling; Thin-walled plate; Composite fibre material

1. Introduction

Dynamic stability of thin-walled structures has been discussed in many works since the 1960's. In the majority of studies numerous simplifications have been made to allow in practice for an effective analysis of stability of the thin-walled structure. Mathematical models tend to aim at higher precision and closer

* Tel.: +48 426 312 221; fax: +48 426 364 985.
E-mail address: tomek@mail.p.lodz.pl

0020-7683/$ - see front matter © 2005 Elsevier Ltd. All rights reserved.
doi:10.1016/j.ijsolstr.2005.02.043

approximation of real structures, which enables one to analyse more and more exactly the phenomena occurring during and after the loss of dynamic stability.

In literature a quantity of "pulse intensity" (Ari-Gur and Simonetta, 1997) or "pulse velocity" (Cui et al., 2001) is introduced. The analysis of dynamic stability of plates under in-plane pulse loading can be divided into three categories depending on pulse duration and magnitude of its amplitude. For pulses of high intensity the impact phenomenon is observed and for pulses of low intensity the problem becomes quasi-static. The dynamic pulse buckling occurs when the loading process is of intermediate amplitude and the pulse duration is close to the period of fundamental natural flexural vibrations (in range of milliseconds). In such case the effects of dumping are neglected.

In world literature one can find many criteria allowing for determination of dynamic critical or failure loads. One of the simplest is the criterion proposed by Volmir (Volmir, 1972), where the dynamic critical load corresponds to the amplitude of pulse force (of constant duration) at which the maximum plate deflection is equal to some constant value k (k—one half or one plate thickness).

In many publications dynamic buckling load is determined on the basis of stability criterion by Budiansky and Hutchinson (Budiansky and Hutchinson, 1966; Hutchinson and Budiansky, 1966), which states that dynamic stability loss occurs when the maximum plate deflection grows rapidly with the small variation of the load amplitude.

Material properties of composites can be freely modelled in selected directions or regions. Thus, it is possible to manufacture structures with variable strength properties. Fibrous composites with properly distributed (concentrated or rarefied) fibres are examples of materials characterised by such properties. Composite materials are most often modelled as orthotropic materials. The structures made of such a material (fibrous composite with varying distribution of fibres) can be very advantageous whenever there is a need for light and strong structures. The thin-walled plate or walls of girders made of fibrous composite with varying distribution of fibres can also be economic because when using the same number of composite fibre (which can be very expensive), it is possible to design such distribution of fibre to obtain the best properties for any kind of load.

In the rich literature devoted to static and dynamic stability problems there are not enough papers dealing with an influence of plate widthwise varying material properties on their behaviour under pulse load and their dynamic stability.

The paper deals with the dynamic response of a thin-walled plate with varying widthwise material properties (stiffness along compression) subjected to in-plane pulse loading of rectangular shape. The problem is investigated on the basis of asymptotic analytical–numerical method and finite element method. The dynamic buckling occurs when the loading process is of intermediate amplitude and the pulse duration is close to the period of fundamental transverse vibrations. Budiansky–Hutchinson criterion of dynamic stability was chosen to determine the critical value of dynamic load factor.

In order to obtain the equations of plate, the non-linear theory of orthotropic thin-walled plates has been modified in such a way that it additionally accounts for all components of inertia forces. The differential equations of motion have been obtained from Hamilton's Principle, taking into account Lagrange's description, full Green's strain tensor for thin-walled plates and Kirchhoff's stress tensor.

2. Formulation of the problem

The rectangular thin-walled composite plate simply supported at both loaded ends and with five different boundary conditions on non-loaded edges is considered. The following boundary conditions on non-loaded edges were considered:

– simply supported on both edges further denoted as *sc1*,
– both edges fixed further denoted as *sc2*,

– one edge simply supported and second fixed further denoted as *sc3*,
– one edge simply supported and second free further denoted as *sc4*,
– one edge fixed and second free further denoted as *sc5*.

The material is subject to Hooke's law. It was assumed that principal axes of orthotropy are parallel to the plate edges (Kolakowski et al., 1999; Kolakowski and Teter, 2000; Kubiak, 2001) and all edges remain straight and parallel during loading.

The plates are made of fibre composite with varying fibre volume fraction widthwise. The analysed material was treated as a homogeneous orthotropic material across the thickness of the plate. Widthwise variable of fibre volume fraction f was assumed as sinusoid function in the following way (Fig. 1):

$$f = f_{\mathrm{av}} + A \cdot \cos\left(\frac{2\pi y}{b}\right), \tag{1}$$

where $f_{\mathrm{av}} = 0.5$ is the assumed average value for fibre volume fraction, A is the sinusoid amplitude defining variation of material properties widthwise plate, with a calculated range of amplitude from -0.4 to 0.4 and b is width of the plate.

In order to determine the magnitude characterising material properties, Eq. (2) found in literature (Kelly, 1989) were used basing on theory of mixture. In both used methods i.e. analytical–numerical and FEM, the analysed plate was divided into 20 bands (Fig. 1) in such a way that each band has different material properties. Using Eq. (2) it is possible to determine an equivalent value for the following material properties:

– modulus of elasticity in longitudinal direction E_{xi} and in transverse direction E_{yi},
– shear modulus G_i,
– Poisson ratio v_{yxi}

which are dependent on fibre volume fraction for ith band.

$$\begin{aligned}
E_{xi} &= E_m(1 - f_i) + E_{\mathrm{f}} f_i;\\
E_{yi} &= E_{\mathrm{m}} \frac{E_{\mathrm{m}}(1 - \sqrt{f_i}) + E_{\mathrm{f}}\sqrt{f_i}}{E_{\mathrm{m}}[1 - \sqrt{f_i}(1 - \sqrt{f_i})] + E_{\mathrm{f}}\sqrt{f_i}(1 - \sqrt{f_i})};\\
v_{yxi} &= v_{\mathrm{m}}(1 - \sqrt{f_i}) + v_{\mathrm{f}}\sqrt{f_i};\\
G_i &= G_{\mathrm{m}} \frac{G_{\mathrm{m}}\sqrt{f_i}(1 - \sqrt{f_i}) + G_{\mathrm{f}}[1 - \sqrt{f_i}(1 - \sqrt{f_i})]}{G_{\mathrm{m}}\sqrt{f_i} + G_{\mathrm{f}}(1 - \sqrt{f_i})}
\end{aligned} \tag{2}$$

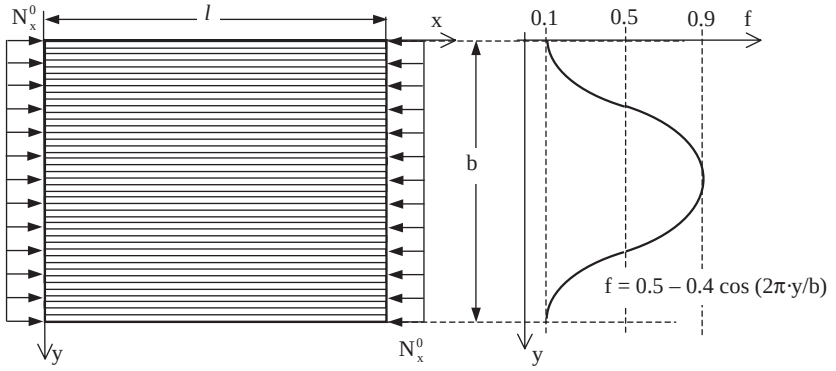

Fig. 1. Band model of a plate with variable fibre volume fraction.

where E_m is the Young's modulus of elasticity for isotropic matrix, E_f is the Young's modulus of elasticity for isotropic fibre, G_m is the shear modulus for isotropic matrix, G_f is the shear modulus for isotropic fibre, v_m is the Poisson's ratio for isotropic matrix, v_f is the Poisson's ratio for isotropic fibre and $f_i = V_f/(V_m + V_f)$ is the fibre volume fraction for ith band.

According to the Betty–Maxwell's theorem the Young's modulus and the Poisson's ratios occurring in Eq. (2) have to satisfy the following relation:

$$E_{ix}v_{iyx} = E_{iy}v_{ixy}. \tag{3}$$

The assumed model of such a plate is built of narrow longitudinal orthotropic bands (plates), and each plate can have a different material properties (Kubiak, 2001). The computational model describes precisely actual structural materials.

A plate model has been assumed. To describe the middle surface strains for each plate band a complete strain tensor for thin plates has been assumed in the form (Kolakowski et al., 1999; Kolakowski and Teter, 2000; Kubiak, 2001):

$$\begin{aligned}
\varepsilon_{ix} &= u_{i,x} + \tfrac{1}{2}(w_{i,x}^2 + u_{i,x}^2 + v_{i,x}^2),\\
\varepsilon_{iy} &= v_{i,y} + \tfrac{1}{2}(w_{i,y}^2 + u_{i,y}^2 + v_{i,y}^2),\\
2\varepsilon_{ixy} &= \gamma_{ixy} = u_{i,y} + v_{i,x} + w_{i,x}w_{i,y} + u_{i,x}u_{i,y} + v_{i,x}v_{i,y},
\end{aligned} \tag{4}$$

where u_i, v_i, w_i-displacements parallel to the respective axes x_i, y_i, z_i of the local Cartesian system of co-ordinates, whose plane $x_i\ y_i$ coincides with the middle surface of the ith plate (ith band) before its buckling (Fig. 2).

The relations which describe the sectional forces and moments reduced to the middle surface of the ith plate (ith band) are written as follows (Kolakowski et al., 1999; Kolakowski and Teter, 2000; Kubiak, 2001):

$$\begin{aligned}
N_{ix} &= \frac{E_i h_i}{1-\eta_i v_i^2}(\varepsilon_{ix} + \eta_i v_i \varepsilon_{iy}),\\
N_{iy} &= \frac{E_i h_i}{1-\eta_i v_i^2}(\eta_i v_i \varepsilon_{ix} + \eta_i \varepsilon_{iy}),\\
N_{ixy} &= N_{iyx} = G_i h_i \gamma_{ixy} = 2G_i h_i \varepsilon_{ixy},\\
M_{ix} &= -D_i(w_{i,xx} + \eta_i v_i w_{i,yy}),\\
M_{iy} &= -\eta_i D_i(v_i w_{i,xx} + w_{i,yy}),\\
M_{ixy} &= -D_{1i} w_{i,xy},
\end{aligned} \tag{5}$$

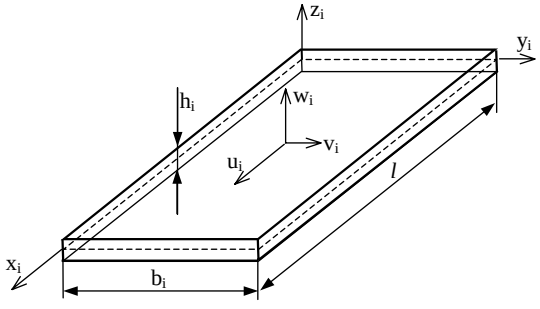

Fig. 2. Dimensions of the ith band of plate and the assumed local co-ordinate system.

where

$$E_i \equiv E_{xi}, \quad \eta_i = \frac{E_{yi}}{E_{xi}} \equiv \frac{E_{yi}}{E_i} = \frac{\nu_{yxi}}{\nu_{xyi}} \equiv \frac{\nu_{yxi}}{\nu_i}, \quad D_i = \frac{E_i h_i^3}{12(1-\eta_i \nu_i^2)}, \quad D_{1i} = \frac{G_i h_i^3}{6}. \tag{6}$$

The differential equations of equilibrium obtained from Hamilton's Principle for a single plate can be written as:

$$\begin{aligned}
&-\rho_i h_i u_{i,tt} + N_{ix,x} + N_{ixy,y} + [(N_{iy}u_{i,y})_{,y} + (N_{ix}u_{i,x})_{,x} + (N_{ixy}u_{i,x})_{,y} + (N_{ixy}u_{i,y})_{,x}] = 0\\
&-\rho_i h_i v_{i,tt} + N_{xyi,x} + N_{yi,y} + [(N_{xi}v_{i,x})_{,x} + (N_{yi}v_{i,y})_{,y} + (N_{xyi}v_{i,x})_{,y} + (N_{xyi}v_{i,y})_{,x}] = 0\\
&-\rho_i h_i w_{i,tt} + (N_{xi,x} + N_{xyi,y})w_{i,x} + (N_{yi,y} + N_{xyi,x})w_{i,y} + N_{xi}w_{i,xx} + N_{yi}w_{i,yy} + 2N_{xyi}w_{i,xy} + M_{xi,xx}\\
&+ 2M_{xyi,xy} + M_{yi,yy} = 0
\end{aligned} \tag{7}$$

The boundary conditions referring to the simply supported ends, i.e. $x = 0$ and $x = \ell$, are assumed to be:

$$\begin{aligned}
&\sum\nolimits_i \int_0^{b_i} N_{xi}(x_i = 0, y_i, t)\mathrm{d}y_i = \sum_i \int_0^{b_i} N_{xi}(x_i = \ell, y_i, t)\mathrm{d}y_i = \sum_i b_i N_{xi0}(t)\\
&v_i(x_i = 0, y_i, t) = v_i(x_i = \ell, y_i, t) = 0; \quad w_i(x_i = 0, y_i, t) = w_i(x_i = \ell, y_i, t) = 0\\
&M_{yi}(x_i = 0, y_i, t) = M_{yi}(x_i = \ell, y_i, t) = 0.
\end{aligned} \tag{8}$$

Let us obtain the equations of motion of a compressed plate assuming that the natural modes of vibration coincide with the buckling modes. Let λ be a load factor, and U-the linear buckling mode with the minimal critical load factor values λ_{cr}. We assume the following expansion of dynamic displacements field (Koiter's type expansion for the buckling problem) (see: (Budiansky, 1974; Sridharan and Benito, 1984; Schokker et al., 1996; Ohga et al., 1998; Kubiak, 2001):

$$\overline{U} \equiv (u, v, w) = \lambda \overline{U}_0 + \xi(t)\overline{U}_1 + \xi^2(t)\overline{U}_2 + \cdots, \tag{9}$$

where ξ is the amplitude of the buckling mode (normalised with the equality condition between the maximum deflection and the thickness of the first plate h_1), $\overline{U}_0$ is the prebuckling static displacement field, $\overline{U}_1$ is the first order displacement field and $\overline{U}_2$ is the second order displacement field.

Similar to the Koiter's theory for the buckling problem (Koiter, 1963), for plate containing geometric imperfections $\bar{u}$ (with only linear initial imperfections determined by the shape of buckling modes), where $\overline{U} = \xi^* U$ the potential energy can be written in the form (Budiansky, 1974; Teter and Kolakowski, 2003):

$$P = \frac{1}{2}a_0\lambda^2 + \frac{1}{2}\xi^2(t)a_1\left(1 - \frac{\lambda}{\lambda_{\mathrm{cr}}}\right) + \frac{1}{3}a_{111}\xi^3(t) + \frac{1}{4}a_{1111}\xi^4(t) - a_1\xi^*\xi(t)\frac{\lambda}{\lambda_{\mathrm{cr}}}, \tag{10}$$

where coefficients a_0, a_1, a_{111}, a_{1111} are determined with the well known formulae (Budiansky, 1974; Kolakowski et al., 1999; Kolakowski and Teter, 2000; Kubiak, 2001; Teter and Kolakowski, 2003) and ξ^* is the amplitude of the imperfection in the form of the buckling mode. Moreover, it was assumed that initial velocity of displacement equals zero $\xi^*_{,t} = 0$.

Neglecting the inertia forces associated with second order inertia terms related to buckling, the kinetic energy with the account of expansion (9) and conditions of orthogonality for U_1 and U_2 is as follows (Budiansky, 1974; Sridharan and Benito, 1984):

$$T = \frac{\rho}{2}\int_0^1 \int_0^b \int_{-\frac{h}{2}}^{\frac{h}{2}} (u_{,t}^2 + v_{,t}^2 + w_{,t}^2)\mathrm{d}x\,\mathrm{d}y\,\mathrm{d}z = \frac{1}{2}m\xi_{,t}^2 \tag{11}$$

Then the Lagrange's equations are:

$$\frac{1}{\omega_0^2}\xi_{,tt}(t) + \left(1 - \frac{\lambda}{\lambda_{cr}}\right)\xi(t) + b_{111}\xi^2(t) + b_{1111}\xi^3(t) - \xi^* \frac{\lambda}{\lambda_{cr}} = 0, \tag{12}$$

where

$$\omega_0^2 = \frac{a_1}{m}; \quad b_{111} = \frac{a_{111}}{a_1}; \quad b_{1111} = \frac{a_{1111}}{a_1}; \quad T_p = \frac{2\pi}{\omega_0}. \tag{13}$$

When the postbuckling behaviour equilibrium path is symmetrical ($a_{111} = 0$), the Lagrange's Eq. (12) can be written as follows:

$$\frac{1}{\omega_0^2}\xi_{,tt}(t) + \left(1 - \frac{\lambda}{\lambda_{cr}}\right)\xi(t) + b_{1111}\xi^3(t) - \xi^* \frac{\lambda}{\lambda_{cr}} = 0. \tag{14}$$

The initial conditions (Sridharan and Benito, 1984; Schokker et al., 1996; Teter and Kolakowski, 2003) are:

$$\xi(t=0) = 0 \quad \text{and} \quad \xi_{,t}(t=0) = 0. \tag{15}$$

The paper takes into account buckling modes for the minimal critical load and the fundamental vibration modes. For more cases critical buckling modes and vibration modes are the same so the solution of eigenvalue problem is searched for various values of mth harmonic (Sridharan and Benito, 1984; Schokker et al., 1996; Teter and Kolakowski, 2003). For the free vibration we set $\lambda = 0$.

The analysed plate was subjected to compression load pulse (Fig. 3). The time of pulse load is equal to natural period T_p.

The system of ordinary differential equilibrium Eq. (7) for the first and the second order approximations is solved by a modified numerical transition matrix method in which the state vector of the final edge is derived from the state vector of the initial edge by numerical integration of the differential equations along the circumferential direction using the Runge–Kutta formulae by means of the Godunov orthogonalization method. Solution of this system in form of trigonometric series was presented in the paper by Kubiak (2001), (see also: Kolakowski et al. (1999), Kolakowski and Teter (2000)).

The equation of motion (12) is solved by the numerical Runge–Kutta method (with step size control and density output).

Consideration of displacements and load components in the middle surface of plates within the first order approximation as well as precise geometrical relationships have enabled the analysis of all possible buckling modes.

The proposed method of solution allows one to take into account an influence of initial imperfections on the free vibration frequency and of critical loads in an easy way (Sridharan and Benito, 1984; Elishakoff et al., 1987).

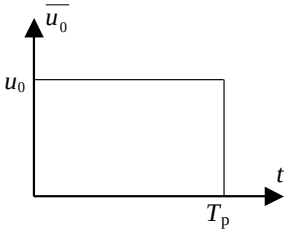

for $0 \le t \le T_p$ $\quad \overline{u_0} = u_0(x = 0, y, t)$

for $t > T_p$ $\quad \overline{u_0} = 0$

where:

$\overline{u_0} = 0$ - load as displacement of loaded plate edge

Fig. 3. Shape of pulse loading.

3. Results of calculated example

Numerical calculations presented in this paper as an example were conducted using own software based on equation presented in paragraph 2. To check the correctness of the obtained results the same cases were calculated using professional software based on finite element method—ANSYS 8.0.

The analysed plate in ANSYS software was divided into four-node shell element (SHELL 43) of six degrees of freedom. The dynamic responses of orthotropic structures loaded by pulse force of rectangular shape with duration T_p were searched for. The analysis in FEM software was divided in two parts. In the first stage the modal analysis and linear stability analysis (eigenvalue method) were performed in order to determine the period of natural frequency T_p, the critical static load λ_{cr} and corresponding buckling mode. In the second stage, buckling eigen-mode with amplitude $\xi^* = 0.01$ as the initial imperfection shape of a plate, pulse force as multiples of the static critical load, and time of acting pulse force equals to the period of natural frequency (T_p), were applied to perform structural dynamic analysis using the "Full Transient Dynamic Analysis".

The applied method allows to find the response of a structure to pulse loading. All examples of the calculation were conducted for pulse compressed rectangular plate ($b = l$) with width to thickness ratio equal $b/h = 100$ for the following boundary conditions:

- simply supported loaded edges;
- five different boundary conditions on longitudinal edges (both simply supported, both fixed, simply supported-fixed, fixed-free edge, simply supported-free edge),

and for variable widthwise fibre volume fraction (1) with amplitude A of sinusoid changing from -0.4 to 0.4.

Epoxy–glass fibre composite was used as an example material for the analysed plate. The material properties for epoxy matrix and glass fibre is presented in Table 1.

The results obtained using both methods (analytical–numerical further denoted as A–N, FEM) from static buckling analysis as a critical force value N_{cr} [N] are presented in Fig. 4 and from modal analysis as a natural frequency (without compression force) ω_0 [Hz] are shown in Fig. 5. Both values presented in Figs. 4 and 5 are shown as a result of function of amplitude A (1), which describes fibre volume fraction widthwise plate.

The coefficient b_{1111} describing the character of the postbuckling equilibrium path obtained from Koiter second order approximation for all analysed plate is shown in Fig. 6 as a function of amplitude A of sinusoid (1).

Figs. 4–6 present the results obtained from analytical numerical method (continuous curve) and from FEM (marks). The obtained results are consistent.

The increase of amplitude A from 0 to 0.4 corresponds to the increase of plate stiffness near the edge of a plate and the decrease of amplitude A from 0 to 0.4 corresponds to the increase of plate stiffness near the middle part of a plate. The results presented in Figs. 4 and 5 show that the increasing stiffness of longitudinal edge of a plate causes an increase of critical buckling load. Similarly the amplitude A causes an

Table 1
Material properties for Epoxy matrix and Glass fibre (Kelly (1989))

	Densityγ[kg/m^3]	Young's modulus E [GPa]	Kirchoff's modulus G [GPa]	Poisson ratio v
Epoxy	1246	3.5	1.25	0.33
Glass	2450	71	30	0.22

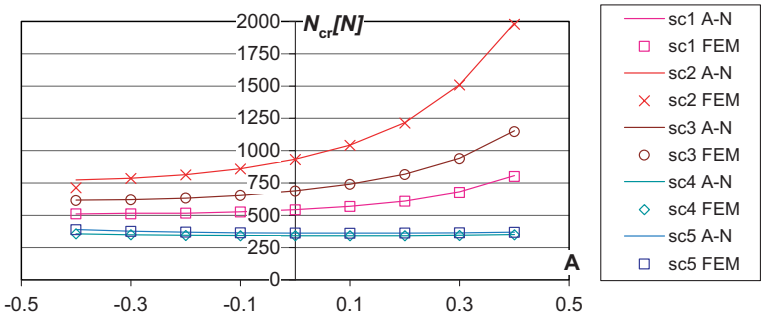

Fig. 4. Critical load value N_{cr} vs. amplitude A.

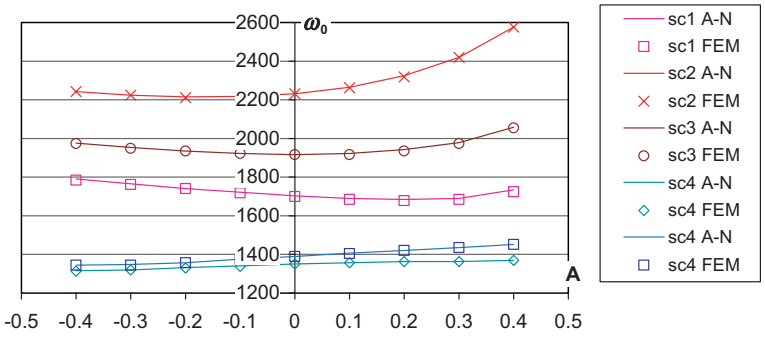

Fig. 5. Natural frequency ω_0 value vs. amplitude A.

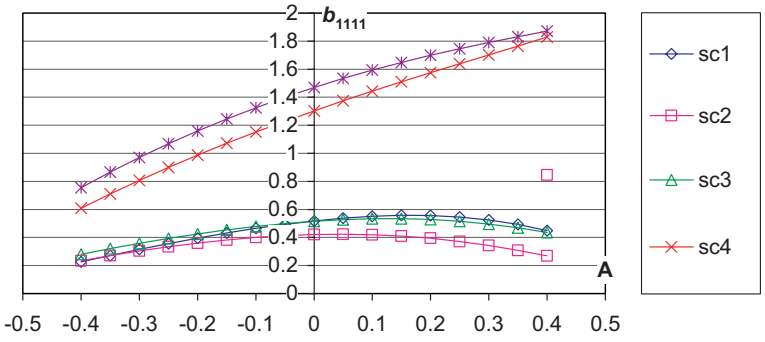

Fig. 6. Coefficient of postbuckling behavior b_{1111} vs. amplitude A.

increase in the value of natural frequencies except the cases denoted as *sc1* (support case 1: simply supported non-loaded edge of plate) and *sc3* (support case 3: one non-loaded edge fixed and second simply supported), in which an increase of amplitude A from 0.4 to 0.2 causes a decrease in the value of natural frequencies and subsequently a very small increase for increasing value of amplitude A to 0.4. For almost all analysed cases the static buckling modes correspond to one half-waves ($m = 1$) in longitudinal direction.

Only for one analysed plate which has a fixed longitudinal edge and material properties corresponding to amplitude $A = 0.4$ the buckling mode has two half-waves in longitudinal direction ($m = 2$). For this case Fig. 6 shows the following results:

– for buckling mode $m = 1$ than $b_{1111} = 0.268$;
– for buckling mode $m = 2$ than $b_{1111} = 0.845$.

Fig. 7 shows a dynamic displacement ξ as a function of dimensionless time t/T_p of the simply supported plates for four values of dynamic load factor $\Lambda = \lambda/\lambda_{cr} = 1.5$; 2.0; 3.0; 4.0 and for impulse duration $T_p = 2\pi/\omega_0$(ω_0—the lowest value of natural frequencies ($m = 1$)) obtained with the FEM (line with sign) and analytical–numerical method (line without sign). In all cases shown in Fig. 7 both used methods give similar results.

Based on maximum value of displacement for different value of dynamic load factor Λ the graphs shown in Figs. 8–12 are prepared. According to the dynamic stability criterion for the impulse duration T_p proposed by Budiansky and Hutchinson for dynamic buckling (Eq. (14)), the value of the dynamic load factor $\Lambda = \lambda/\lambda_{cr}$ can be found from graphs presented in Figs. 8–12. As it is shown in these graphs the critical value of dynamic load factor Λ_{cr} depends on b_{1111} value. For the analysed cases the maximum value of critical dynamic load factor is obtained for a plate with a stiffened middle part of a plate (amplitude $A = -0.4$). The minimum value of Λ_{cr} is obtained for a plate with nearly uniform distributed fibre volume fraction widthwise plate ($A = 0.1$ to 0.15) for boundary condition cases denoted as *sc1*, *sc2* and *sc3*. For the cases of boundary condition with free edges the critical value of Λ_{cr} decreases with an increasing value of post-buckling coefficient b_{1111}.

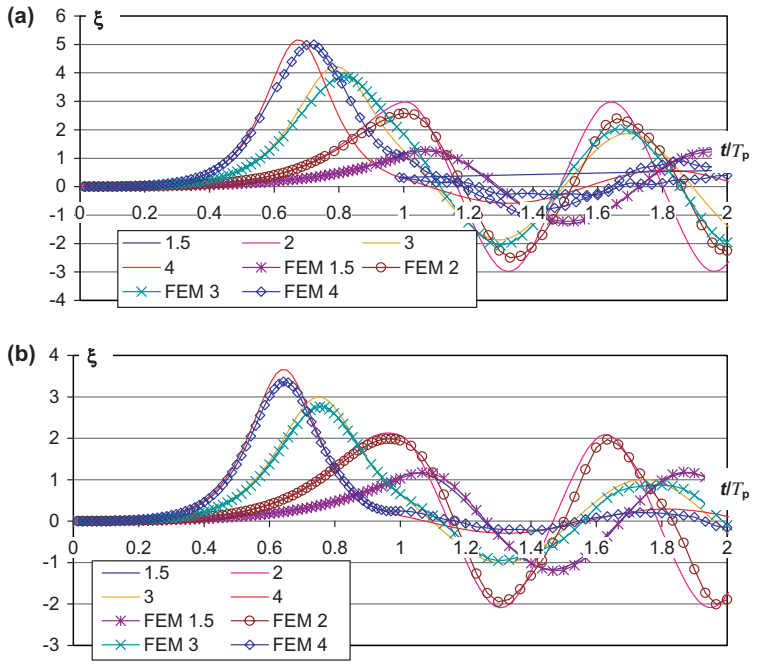

Fig. 7. Comparison of dynamic deflection obtained with the FEM and analytical–numerical method for simply supported plate and $A = -0.4$(a); 0.4(b).

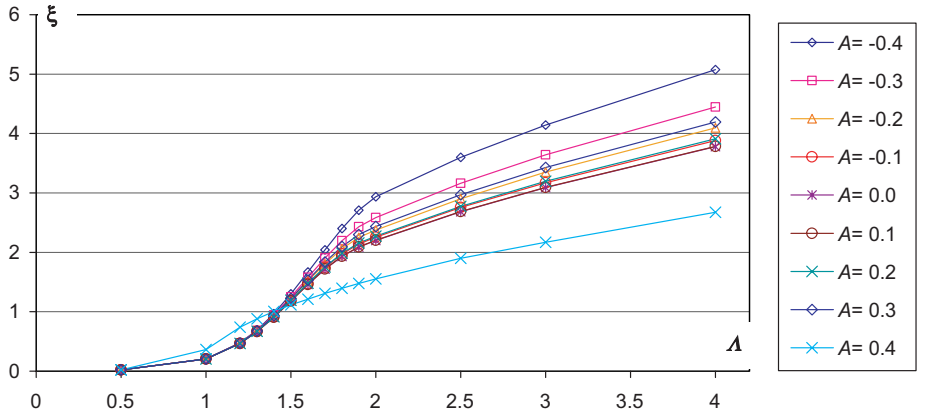

Fig. 8. Dimensionless displacement ξ vs. dynamic load factor Λ for case denoted as *sc1*.

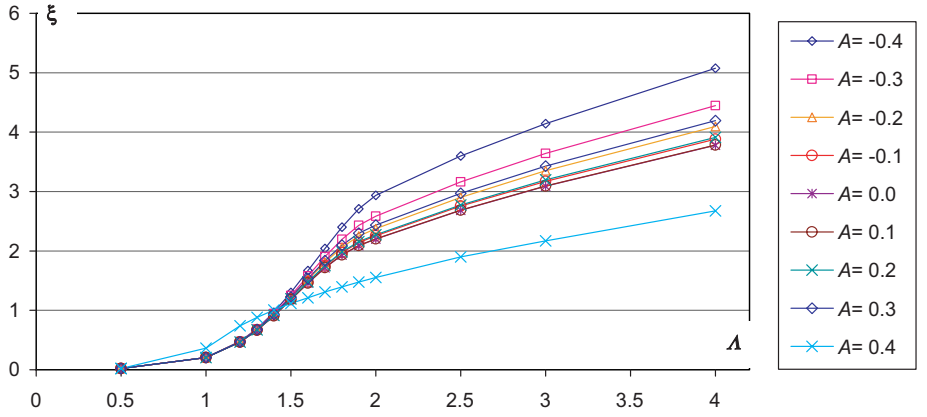

Fig. 9. Dimensionless displacement ξ vs. dynamic load factor Λ for case denoted as *sc2*.

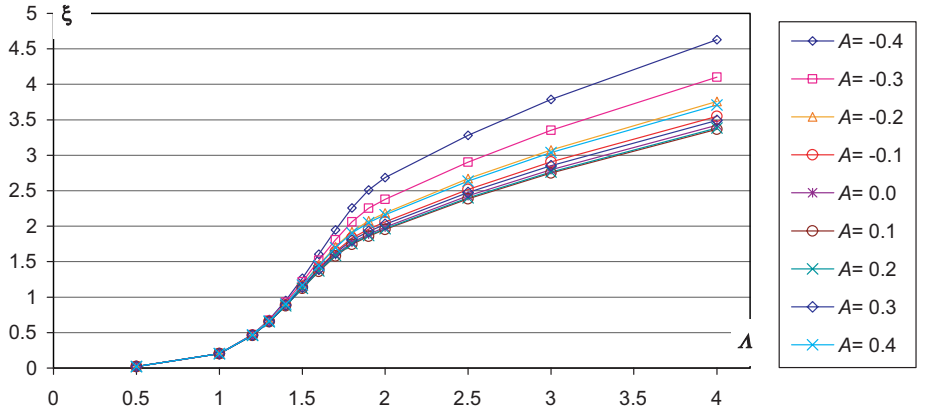

Fig. 10. Dimensionless displacement ξ vs. dynamic load factor Λ for case denoted as *sc3*.

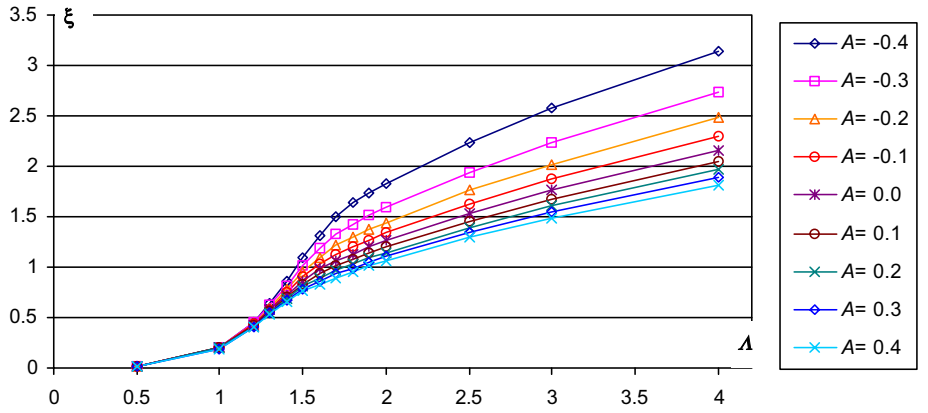

Fig. 11. Dimensionless displacement ξ vs. dynamic load factor Λ for case denoted as *sc4*.

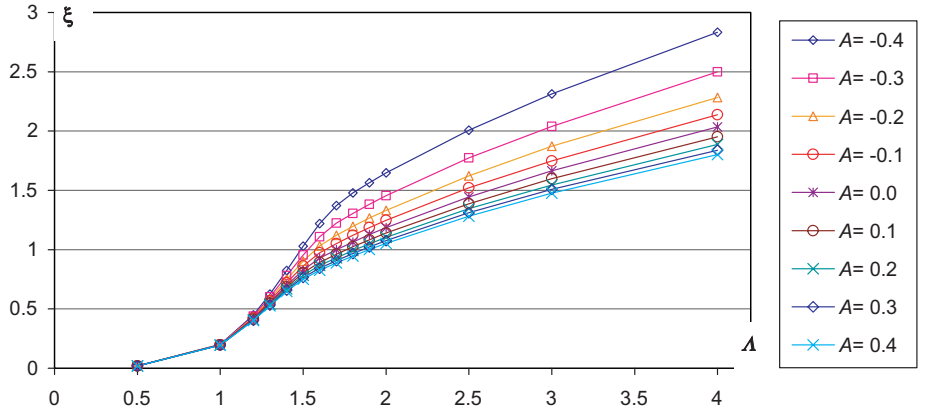

Fig. 12. Dimensionless displacement ξ vs. dynamic load factor Λ for case denoted as *sc5*.

Fig. 13 shows a dynamic displacement ξ as a function of dimensionless time t/T_p for the boundary condition case denoted as *sc2* (fixed non-loaded edges) and for the amplitude $A = 0.4$. In this case the buckling mode for the critical value of compressed force is a mode with two half-waves ($m = 2$). For this case the dynamic buckling analysis was performed with initial imperfection ($\xi^* = 0.01$) corresponding to buckling mode ($m = 2$) for minimal critical value and for the impulse duration T_p calculated from the lowest value of natural frequencies ($m = 1$). The curves shown in Fig. 13 were obtained with the FEM and analytical–numerical method for four values of dynamic load factor $\Lambda = 1.0$; 2.0; 3.0 and 4.0. The results obtained using both method are similar for $\Lambda = 1.0$ during the whole analysed time and for the remaining analysed Λ during the time when displacement increased from zero to maximum value (first part of curves $\xi(t/T_p)$). Differences between results obtained from both methods are very well visible for $\Lambda = 3.0$ and $\Lambda = 4.0$ for $t/T_p > 0.7$ (Fig. 13). The reason for the differences in the obtained results is a changeable number of half-waves which can only be analysed with FEM, because in proposed analytical–numerical method it is assumed that the number of half-waves during dynamic analysis does not change.

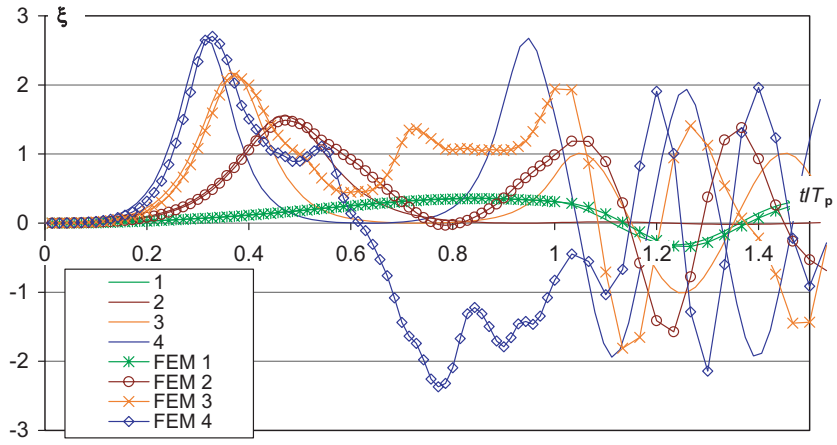

Fig. 13. Comparison of dynamic deflection obtained with the FEM and analytical–numerical method for fixed longitudinal edge of the plate and $A = 0.4$ for $m = 2$.

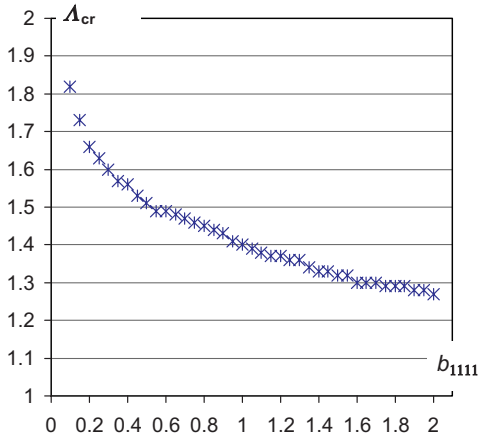

Fig. 14. Influence of postbuckling coefficient b_{1111} on critical value of dynamic load factor Λ_{cr}.

For cases in which the number of half-waves in the longitudinal direction is $m = 1$ it is possible to prepare graphs (Fig. 14) showing the influence of postbuckling coefficient b_{1111} on the critical value of dynamic load factor Λ_{cr} for initial imperfection $\xi^* = 0.01$.

4. Conclusion

The results of numerical calculation obtained from FEM and proposed analytical–numerical method were similar in all analysed cases. Only in cases for which the buckling mode (number of half-waves) varies during and after impulse of load (case denoted as *sc2* for $A = 0.4$ and $\Lambda > 2$) the results obtained using both methods were different (Fig. 13). The differences in results come from the fact that the proposed method does not allow to analyse the change of buckling modes over time progress. Nevertheless the cases with

different results were obtained for deflection load factor greater than two and according to Budiansky–Hutchinson criterion the critical value of dynamic load factor Λ_{cr} for this case was found in range $1 < \Lambda < 1.5$ (Fig. 9). In spite of differences in results obtained using both method for deflection load factor $\Lambda > 2$ and for time greater then time corresponding to maximal displacement, proposed analytical–numerical method of analysis of the dynamic buckling gives positive results because this method bases on criterion proposed by Budiansky–Hutchinson in which only the maximal value of deflection ξ is used.

The advantage of the proposed method of finding Λ_{cr} for analysed plate in comparison with FEM is time of calculation. The time of obtaining one curve $\xi(T_p)$ (Fig. 13) using analytical–numerical method averages 20 s, while using FEM the time of calculation averages 1.5 h. The times of calculation were obtained on PC computer with Pentium 4. The advantage of FEM is postprocessing (very good tools for presenting calculated results) and FEM gives possibility to analyse more complicated structures than plates with widthwise varying material properties.

References

Ari-Gur, J., Simonetta, S.R., 1997. Dynamic pulse buckling of rectangular composite plates. Composites Part B 28, 301–308.

Budiansky, B., Hutchinson, J.W., 1966. Dynamic buckling of imperfection-sensitive structures. In: Goetler H. (Ed.), Proceedings of the Eleventh International Congress of Applied Mechanics, Munich, pp. 636–651.

Budiansky, B., 1974. Theory of buckling and post-buckling behaviour of elastic structures. Advances in Applied Mechanics, Vol. 14. Acad. Press, pp. 1–65.

Cui, S., et al., 2001. Dynamic buckling and collapse of rectangular plates under intermediate velocity impact, In: Proceedings of Third International Conference of Thin-Walled Structures, Cracow, pp. 365–372.

Elishakoff, I., Birman, V., Singer, J., 1987. Small vibrations of an imperfection in the vicinity of a nonlinear static state. Journal of Sound and Vibration 114, 57–63.

Hutchinson, J.W., Budiansky, B., 1966. Dynamic buckling estimates. AIAA Journal 4-3, 525–530.

Kelly, A. (Ed.), 1989. Concise Encyclopedia of Composite Materials. Pergamon Press.

Koiter, W.T., 1963. Elastic stability and post-buckling behaviour. In: Proceedings of the Symposium on Nonlinear Problems, Univ. of Wisconsin Press, Wisconsin, pp. 257–275.

Kolakowski, Z., Kowal-Michalska, K., 1999. Selected Problems of Instabilities in Composite Structures. A Series of Monographs. Technical University of Lodz, Poland.

Kolakowski, Z., Teter, A., 2000. Interactive buckling of thin-walled beam-columns with intermediate stiffeners or/and variable thickness. International Journal of Solids and Structures 37 (24), 3323–3344.

Kubiak, T., 2001. Postbuckling behaviour of thin-walled girders with orthotropy varying widthwise. International Journal of Solids and Structures 38, 4839–4855.

Ohga, M., Nishimoto, K., Shigematsu, T., Hara, T., 1998. Natural frequencies and modes shapes of thin-walled members under in-plane forces. Thin-Walled Structures. Research and Development. In: 2nd International Conference on Thin-Walled Structures, Singapore, pp. 501–508.

Schokker, A., Sridharan, S., Kasagi, A., 1996. Dynamic buckling of composite shells. Computers and Structures 59 (1), 43–55.

Sridharan, S., Benito, R., 1984. Columns Static and Dynamic Interactive Buckling. Journal of Engineering Mechanics, ASCE 110-1, pp. 49–65.

Teter, A., Kolakowski, Z., 2003. Natural frequencies of a thin-walled structures with central intermediate stiffeners or/and variable thickness. Thin-Walled Structures 41, 291–316.

Volmir, S.A., 1972. Nonlinear Dynamics of Plates and Shells. Science, Moscow (in Russian).